Title
Conceptual design and configuration performance analyses of polygenerating high temperature fuel cells

Journal
International Journal of Hydrogen Energy, 36(16)

ISSN
0360-3199

Authors
Margalef, P
Brown, T
Brouwer, J
et al.

Publication Date
2011-08-01

DOI
10.1016/j.ijhydene.2011.05.072

Available at www.sciencedirect.com

ScienceDirect

journal homepage: www.elsevier.com/locate/he

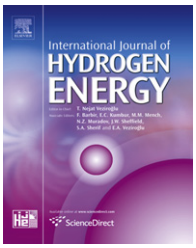

Conceptual design and configuration performance analyses of polygenerating high temperature fuel cells

Pere Margalef, Tim Brown, Jacob Brouwer, Scott Samuelsen*

National Fuel Cell Research Center, University of California, Irvine, USA

ARTICLE INFO

Article history:
Received 22 February 2011
Received in revised form
29 April 2011
Accepted 11 May 2011
Available online 23 June 2011

Keywords:
High temperature fuel cell
Polygeneration
Hydrogen
Efficiency
System Configuration

ABSTRACT

The use of a high temperature fuel cell (HTFC) to continuously and simultaneously polygenerate hydrogen in combination with electricity and heat represents a promising technology as a source of fuel for fuel cell vehicles. Different configurations of polygenerating HTFC, including different designs with internal and external reforming are options to polygenerate electricity, hydrogen and heat. The current study analyzes and compares six different configurations based on solid oxide technology. Efficiency results based upon the Supplemental Input Method demonstrate that internal reforming configurations achieve higher performance than when hydrogen product is produced in an external reformer. The overall efficiency and the efficiency in the generation of each product are used as the basis for comparison.

1. Introduction

It has been suggested that hydrogen fuel may become the petroleum product's replacement for fueling automobiles to reduce carbon dioxide and criteria pollutant emissions, and eliminate dependence on oil [1]. Hydrogen is widely used in the chemical industry for making nitrogen fertilizers and upgrading crude oils into transport fuels [1]. Worldwide hydrogen demand in refineries and chemical plants is equivalent to roughly 200 GW of thermal energy [1]. In addition, depletion of fossil fuels motivates the use of hydrogen in transportation which is expected to drastically increase the demand of hydrogen. Fuel cell technology is a preferred alternative for the transportation sector due to its higher efficiency than internal combustion engines, operation with zero pollutant or greenhouse gas emissions, multiple production methods and feedstock, and capability to power vehicles over 300 miles on a single 3-min fueling [2].

Unfortunately, hydrogen is not naturally occurring on earth and it has to be produced from other resources. There are several energy sources that can be used to produce hydrogen such as nuclear, renewables, and fossil fuels. Hydrogen production processes can be classified into thermochemical and electrochemical processes. Thermochemical processes for hydrogen production involve thermally assisted chemical reactions that release hydrogen from hydrocarbon fuels or water. The most common thermochemical process for hydrogen production is steam methane reforming (SMR) [3]. This technology is very mature and efficient but involves hydrocarbon feedstock which may be seen as a downside in terms of energy security and climate change. Alternative thermochemical processes split water into hydrogen and oxygen through a series of thermally driven reactions. This

* *Corresponding author*. Tel.: +1 949 824 1999x221; fax: +1 949 824 7423.
E-mail address: jb@nfcrc.uci.edu (J. Brouwer).
0360-3199/$ – see front matter
doi:10.1016/j.ijhydene.2011.05.072

process is called thermochemical water splitting and is possible through the very high temperature potential of solar or nuclear sources.

Electrochemical processes involve electrolysis of water or steam that leads to decomposition of water into hydrogen and oxygen. It is a proven and currently commercial technology. However, it involves high electricity consumption that increases the cost of the hydrogen compared with thermochemical processes. In addition, unless the electricity is produced with carbon-free technology such as renewables, hydrogen production via electrolysis also leads to a significant carbon footprint. One promising solution to couple renewable technology such as wind and solar, with hydrogen production is to produce hydrogen when there is an electricity production surplus as a means of energy storage and fuel production. Significant efforts are already in place and it is expected that as renewable technologies penetrate into the energy mix, significant portions of hydrogen will be produced via this method [4].

Similarly to the use of surplus renewable electricity to produce hydrogen via electrochemical processes, there is also the possibility to produce hydrogen via thermochemical processes by recovering waste heat from conventional power generation devices. Yildiz and Kazimi investigated the production of hydrogen from nuclear energy technologies [1]. In their work, they investigated the coupling of different thermochemical and electrochemical hydrogen production processes with alternative nuclear energy technologies. Similarly, Brouwer and Leal investigated the production of hydrogen by coupling high temperature fuel cells with a steam methane reformer. Brouwer and Leal [5] analyzed and compared eight different cycle configurations using solid oxide fuel cells (SOFC) and molten carbonate fuel cells (MCFC). Six of the eight configurations use fuel cell heat to drive hydrogen production in an external reformer placed in different positions in the cycle. The other two configurations use the internal reformation capabilities of SOFC to produce hydrogen.

The work herein presented investigates in detail how placing the external reformer in different positions affects the fuel cell performance and the hydrogen production efficiency. The methodology used is based on detailed thermodynamic and electrochemical principles that apply to each of the system components and the integrated cycles. Temperature, gas composition and enthalpy are calculated for each state point. As a result, fuel cell performance as well as hydrogen production potential has been evaluated for each configuration.

While Brouwer and Leal's work [6] studied SOFC and MCFC cycles, this study analyzes only SOFC technology. Additionally, the current work evaluates system operation at different fuel utilizations to investigate the synergies associated with lower utilization factors after the work of Margalef [7]. Additionally, this analysis incorporates the hydrogen separation and purification process into the system configuration and investigates the effects of coproducing hydrogen on the fuel cell performance (i.e., cell voltages). Finally, a comparative analysis of each configuration based upon the efficiency calculation methodologies developed by Margalef et al. [8] is provided in order to determine the most efficient polygenerating HTFC configuration.

2. Hydrogen production with high temperature fuel cells

High temperature fuel cells (HTFC) generate electricity and heat through exothermic electrochemical reactions. Oxidation of hydrogen takes place in the anode compartment and is described by the overall hydrogen oxidation reaction

$$H_2 + \frac{1}{2}O_2 \rightarrow H_2O(\text{steam}) \quad \Delta H = -241.83 \text{ kJ mol}^{-1} \tag{1}$$

This reaction occurs at the triple-phase boundary where hydrogen is adsorbed and undergoes the oxidation half-reaction as follows

$$H_2 + O^{2-} \rightarrow H_2O + 2e^- \tag{2}$$

The electrons released flow through the external circuit to produce the desired useful electrical power. On the cathode side, oxygen is adsorbed and reduced by the arriving electrons according to the half-reaction

$$\frac{1}{2}O_2 + 2e^- \rightarrow O^{2-} \tag{3}$$

Oxygen ions are conducted through the electrolyte from the cathode to the anode to perpetuate the electrochemical reactions.

Generated heat by the exothermic fuel cell reactions is typically utilized internally or externally by the endothermic fuel processing reactions, which in turn provides cooling to the system [9]. Surplus heat is used to preheat the fuel and oxidant streams before they enter the fuel cell and to produce the steam required for system operations. In addition, the remaining thermal energy contained in the exhaust gases can be used downstream of the fuel cell for polygeneration applications that require or value heat [10].

One possible configuration is to use the fuel cell heat to produce hydrogen via steam methane reforming in an external reformer (i.e., external reformation). Another possibility relies on the internal reforming capabilities of HTFCs and on the fact that the amount of high quality heat produced by the exothermic reactions within the stack is typically much greater than that heat required for fuel processing [13]. Therefore, more hydrocarbon fuel than that required for the electricity generation could be processed in an HTFC, creating a hydrogen-rich stream that could be subsequently purified and delivered at the point of production without the need of an external reformer [9] (i.e., internal reformation). This mode of operation implies lower stack fuel utilization factors and has been associated with synergies such as lower cell polarization losses and lower parasitic losses correlated with lower cooling air requirements [7].

If successfully developed, polygenerating HTFC that produce electricity, heat and hydrogen from a wide variety of hydrocarbon fuels will provide a distributed generation facility for hydrogen that would facilitate the development of fueling infrastructure for fuel cell vehicles. In addition, such a concept could aid fuel cell market viability, stakeholder

confidence, and energy security and sustainability as well as environmental emissions reduction [7].

2.1. System configurations based upon the fuel processing

In high temperature fuel cells, Steam Methane Reformation (SMR) and Water-Gas Shift (WGS) are the main fuel processing reactions that convert raw fuel (i.e., natural gas) into fuels more amenable to electrochemical oxidation (i.e., hydrogen and carbon monoxide).

Steam Methane Reforming consists of the reaction of methane and steam over a supported nickel catalyst to produce a mixture of hydrogen, carbon monoxide, carbon dioxide and methane. The basic reforming reaction for methane is

$$CH_4 + H_2O \rightarrow 3H_2 + CO \quad \Delta H = 206 \text{ kJ mol}^{-1} \tag{4}$$

Steam reformation is an endothermic reaction. Heat has to be provided to drive the reaction forward to the hydrogen production direction. Fig. 1 shows the equilibrium composition of steam methane reformation reactants and products as a function of temperature. As observed, the hydrogen concentration is highest between 900 K and 1100 K [11].

The water-gas shift (WGS) reaction (starting from steam) is slightly exothermic and occurs at the same time as steam reforming [12]. During the shift reaction, additional hydrogen is produced. The basic water-gas shift reaction for carbon monoxide is

$$CO + H_2O_{(g)} \rightarrow H_2 + CO_2 \quad \Delta H = -41 \text{ kJ mol}^{-1} \tag{5}$$

2.1.1. External reformation configurations

In this work, five different configurations based on the designs analyzed by Brouwer and Leal [5] are evaluated. In all cases, steam reformation is driven by the fuel cell exhaust heat in an external reformer, which takes as much heat as possible without compromising the fuel cell operating temperatures. Differently than Brouwer and Leal's work, the inlet temperature of the fuel, steam and air streams are kept constant at 1173 K in order to sustain the electrochemical reactions within the stack. Therefore, depending on the external reformer location, more or less heat is available to produce hydrogen with the external reformer. Figs. 2–6 illustrate the schematics of the external reformation configurations. Note that in all the configurations, a hydrogen separation unit (HSU) block, based on PSA technology, is placed downstream of the reformer to separate and purify the hydrogen stream from the reformate gas. Hydrogen separation and purification is relatively energy intensive. Therefore, this modeling effort incorporates the capabilities of estimating the parasitic loads associated with the hydrogen separation and purification processes for each configuration.

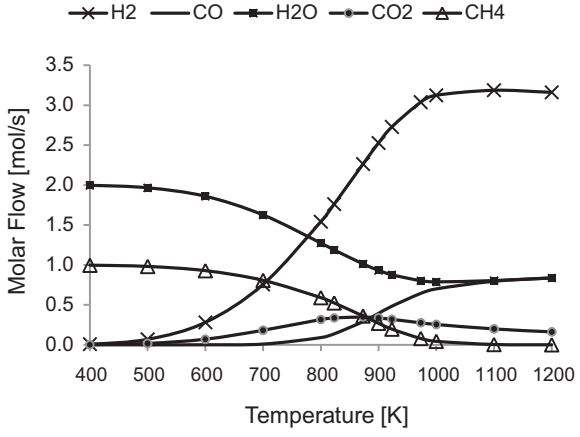

Fig. 1 – Equilibrium composition as a function of temperature (steam-to-carbon ratio S/C = 2) [6].

2.1.2. Internal reformation configurations

Internal reforming promotes hydrogen production within the fuel cell stack and provides cooling to the fuel cell stack due to its endothermic nature. Generally, fuel cell systems do not electrochemically consume all the fuel that is supplied (a fundamental limitation for all fuel cells) and they produce enough heat to reform much more fuel than the amount they consume. Remaining fuel exiting the anode presents a unique opportunity for low cost hydrogen [7].

One internal reformation SOFC configuration at two fuel utilization (U_F) values is studied (Configurations 6a/b). The analyzed fuel utilization factors are 80% and 60%, respectively. Fig. 7 shows the schematics of this configuration. As seen, the HSU block is placed at the anode gas exit so hydrogen is separated from the anode-off-gas before it is oxidized in the catalytic combustor.

Because of the low electric resistance of the bipolar plates and the electrodes, it is not possible for different parts of a single cell to have different voltages. This characteristic of an electrode is often referred to as an equipotential surface [13]. As a result, current density varies along the cell, being lowest near the fuel outlet because the reactant concentration is lower at this point. As reactants circulate through the anode and cathode, they are consumed by the cell electrochemistry reducing their concentration along the cell. When the concentration drops, partial pressure drops as well. Analyzing the Nernst equation, it can be concluded that reactant depletion in the anode compartment reduces the Nernst Voltage V_{Nernst}.

$$V_{Nernst} = E_0 + \frac{RT}{2F}\ln\left(\frac{p_{H_2}p_{O_2}^{\frac{1}{2}}}{p_{H_2O}}\right) \tag{6}$$

where E_0 is the ideal reversible potential, F is Faraday's constant [96,487 kC/kmol], and p_k is the partial pressure of the element k [14]. E_0 s defined by the following expression

$$E_0 = \frac{-\Delta g_f(T)}{2F} \tag{7}$$

where $-\Delta g_f(T)$ is the change in Gibbs free energy as a function of temperature.

Note that if the fuel or oxidant species concentrations become completely depleted (zero) then the Nernst potential cannot be sustained. If this happens anywhere along the highly conductive electrode surface (equipotential surface) then the cell voltage cannot be sustained. Therefore, the

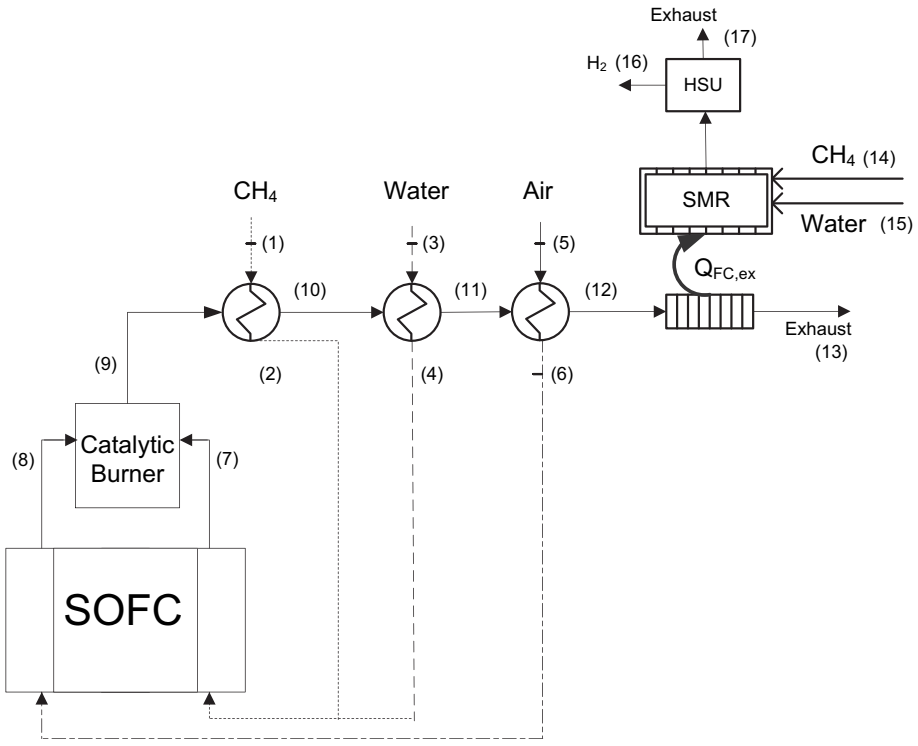

Fig. 2 – Configuration 1: SOFC, external reformation after the air preheater; (U_F: 80%).

amount of fuel and oxidant fed into the fuel cell must be greater than the amount consumed within the stack at all times. In this way, current densities will be kept high and relatively constant along the entire length of a cell [13]. Importantly, Nernst voltage drop will be largest in high temperature fuel cells resulting from the RT term from Eq. (3).

3. Approach and methodology

To evaluate the fuel cell performance and the hydrogen production capabilities with each configuration, a steady-state polygenerating HTFC model has been developed. The

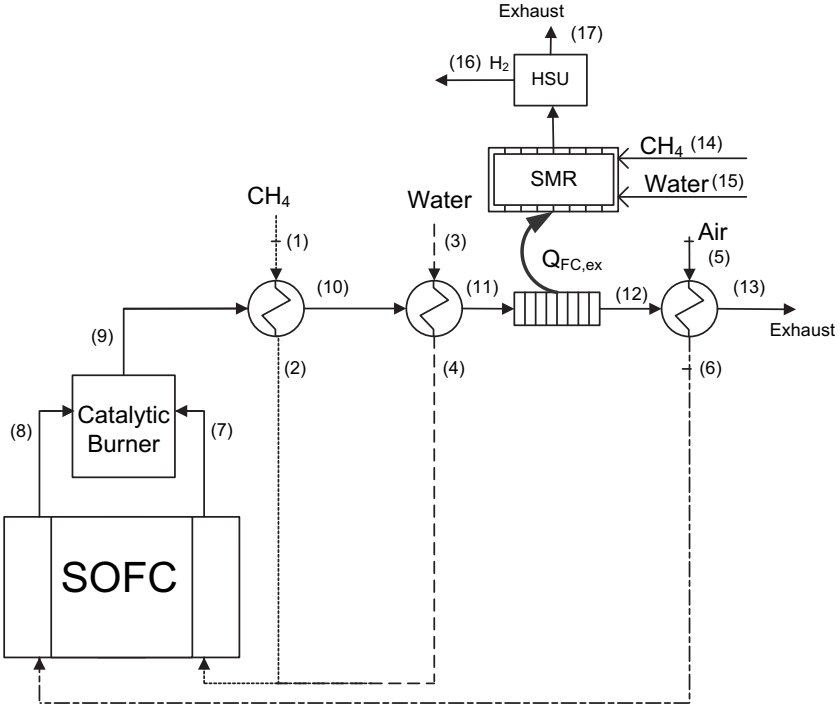

Fig 3 – Configuration 2: SOFC, external reformation after the water preheater; (U_F: 80%).

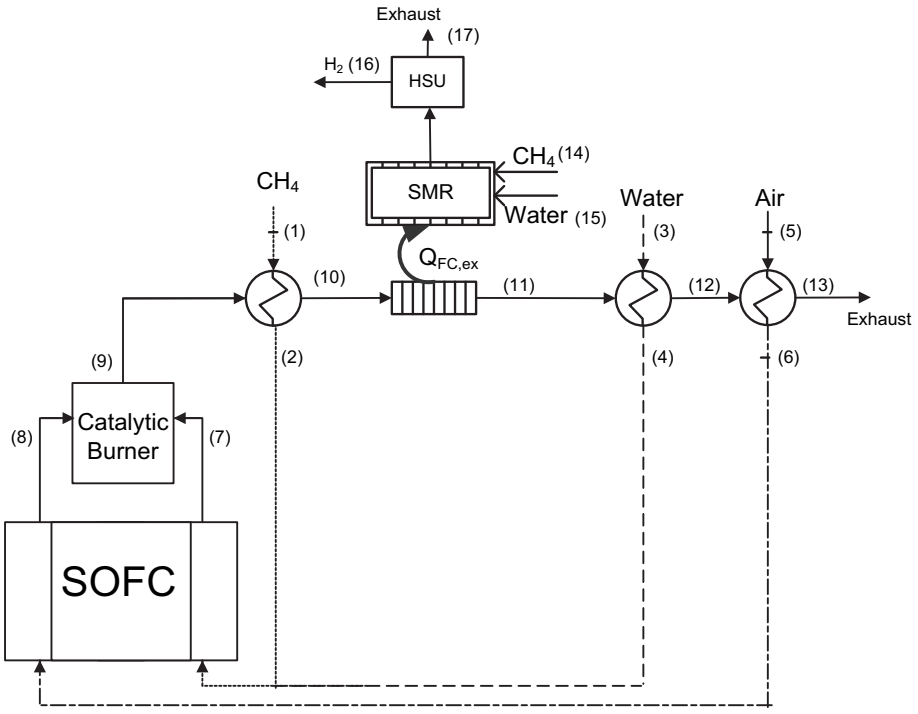

Fig 4 – Configuration 3(a/b): SOFC, external reformation after the fuel preheater; (U_F: 80%/60%).

complete model consists of a SOFC stack; heat exchangers to preheat the fuel, water and air; an external SMR reactor placed in different locations consisting of the different configurations; an adiabatic catalytic combustor that captures the thermal energy of the unused fuel downstream the stack; and a Hydrogen Separation Unit (HSU) block based on PSA technology.

In configurations 1 to 4, the adiabatic catalytic burner is placed after the anode and cathode compartments. As seen in Figs. 2–5, the external reformer is placed at different locations in between the heat exchangers leading to the different configurations.

Shown in Fig. 6, configuration 5 is different than the previous configurations since the adiabatic catalytic burner is

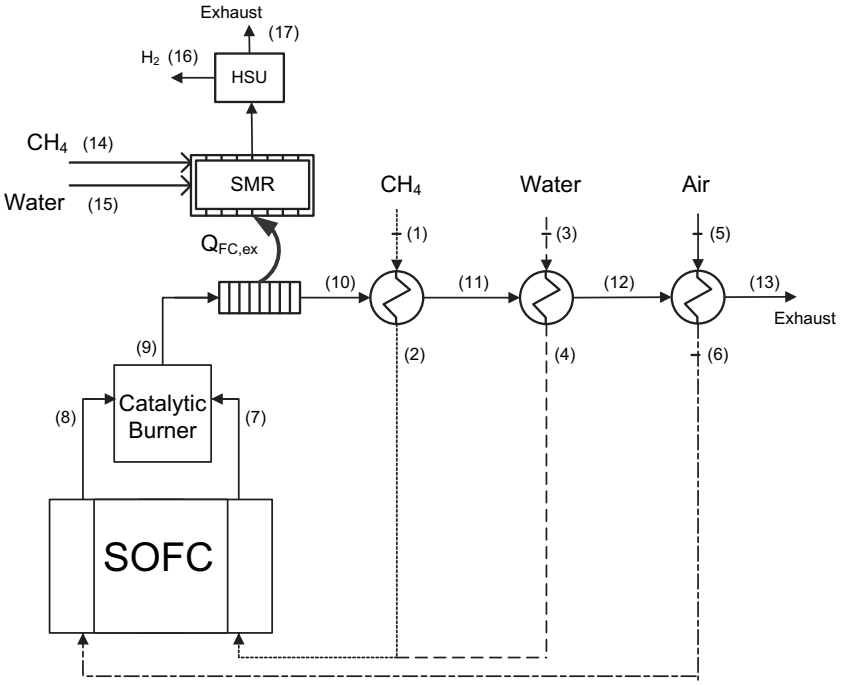

Fig. 5 – Configuration 4: SOFC, external reformation after the catalytic burner; (U_F: 80%).

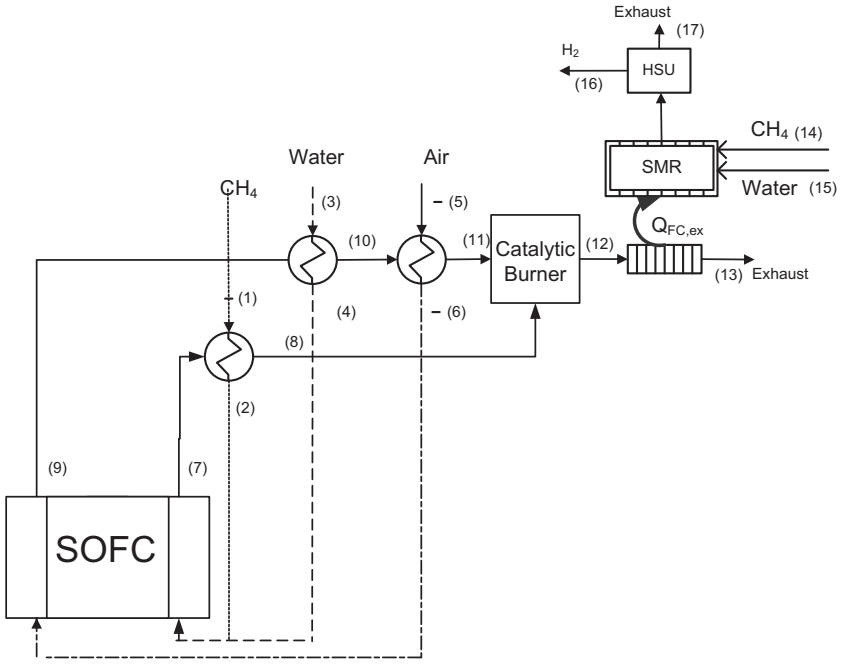

Fig. 6 – Configuration 5: SOFC, burner and external reformation after preheaters; (U_F: 80%).

located after the heat exchangers. Cathode exhaust gas is used to preheat the water and the air whereas the anode-off-gas is used to preheat the fuel. Both anode and cathode exhaust gases react in the catalytic burner. The external reformer captures the heat from the catalytic combustor exhaust stream.

Configuration 6 does not contain an external reformer, as seen in Fig. 7. Instead, the unused hydrogen in the anode-off-gas is separated before it enters the catalytic burner.

Each configuration has been analyzed following the same approach. For the external reformation cases (Conf. 1–5), stack input temperatures of the fuel, air and steam have been fixed at 1173 K whereas the amount of reformed methane varies depending on how much heat is available after preheating all the input streams. Pinch analyses for each heat exchanger have been performed in order to avoid temperature crossovers within the heat exchangers. Similarly, for the internal reformation cases (Conf. 6a/6b), the amount of hydrogen extracted in the HSU block depends upon how much thermal energy has to be extracted from the anode-off-gas in order to preheat the input streams to the specified temperatures.

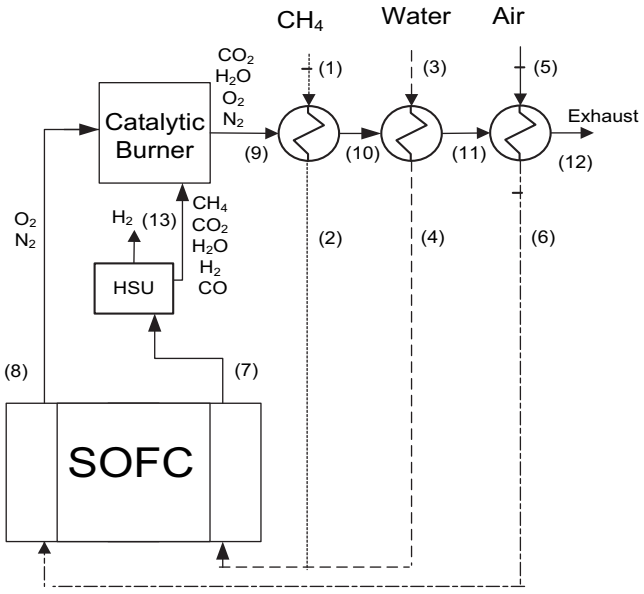

Fig. 7 – Configuration 6(a/b): SOFC, internal reformation; (U_F: 80%/60%).

3.1. *Model overview*

For this work, a steady-state solid oxide fuel cell, external reformer and hydrogen separation unit based on PSA technology have been modeled and integrated in different configurations. The required model inputs are:

- Fuel cell power capacity [kW]
- Fuel utilization factor in the anode side [%]
- Fuel composition and steam-to-carbon ratio
- Air utilization factor in the cathode side [%]
- Fuel, air and steam fuel cell input temperatures [K]

The model generates the following information for each of the configurations:

- Reversible open circuit and Nernst voltage [V]
- Net electric power [kW]
- Hydrogen produced [kg/h]
- Parasitic loads associated with hydrogen purification (i.e., PSA) [kW]
- Fuel cell stack and external reformer bulk temperatures [K]

- Exhaust gas temperature [K]
- Equilibrium composition of each stream
- Overall polygeneration efficiency [%]
- Fuel cell electrical efficiency [%]
- Hydrogen production efficiency [%]

3.2. Chemical equilibrium and thermodynamic analysis

Steam methane reforming occurs within the external SMR reactor as well as within the solid oxide fuel cell anode compartment (i.e., internal reformation). Both cases have been analyzed assuming chemical equilibrium to predict the equilibrium composition as a function of the temperature and pressure. There are two methods to state chemical equilibrium. The first one uses equilibrium constants, the second one, as used for this analysis, is based on the minimization of the Gibbs free energy. For a given temperature and pressure, the equations for the species conservation, atoms conservation and condensed species are

$$N = \sum_{k=1}^{m} N_k \quad k = 1, \ldots, m \tag{8}$$

$$b_l^0 = \sum_{k=1}^{m} a_{lk} N_k = b_l \quad l = 1, \ldots, l \tag{9}$$

$$\frac{\mu_k^0}{R_u T} + \sum_{l=1}^{t} \left(\frac{\lambda_l}{R_u T}\right) a_{lk} = 0 \quad k = m+1, \ldots, n \tag{10}$$

Where N is the molar flow [kmol/s], b_l^0 is the number of atoms of element I in the reactants [kmol], a_{lk} is the number of atoms of element I in the species k in the product [kmol], μ_k^0 is the molar chemical potential of species k in the reactants [kJ/kmol], λ_l is a Lagrange multiplier, and R_u is the universal gas constant. Equations (8) to (10) form a set of n+1 equations that can be simultaneously solved for the unknowns N_k,λ_l and N. The thermodynamic function is then solved by the Newton–Raphson method for the unknowns [15].

3.3. Solid oxide fuel cell equilibrium model

The following considerations and assumptions have been used for the fuel cell model

- Fuel, air and steam streams are preheated to 1173 K before entering the fuel cell stack by the fuel cell exhaust gas.
- Internal reformation occurs within the fuel cell stack (Direct internal reformation)
- Fuel cell electrical output is 1 MW.
- Considered fuel utilizations (U_F) are 80% and 60%, depending on the configuration.
- Oxidant utilization are 25% and 15% depending on the configuration.
- Activation (η_{act}), ohmic (η_{ohm}), and concentration (η_{con}) losses are negligible.
- All gas stream pressures are slightly higher than atmospheric pressure
- Anode-off-gas is at chemical equilibrium

Thus, the fuel cell voltage is approximately equal to the Nernst Voltage defined by Eq. (6).

$$V_{cell} = V_{Nernst} - \eta_{act,an} - \eta_{act,ca} - \eta_{ohm} - \eta_{conc} \sim V_{Nernst} \tag{11}$$

3.4. External reformer equilibrium model

Configurations 1 to 5 generate hydrogen with an external reformer linked to a heat exchanger that takes as much heat as possible from the fuel cell exhaust stream ($Q_{FC,ex}$). Heat from the fuel cell exhaust is taken without compromising the overall thermal balance. The amount of additional methane fed into the external reformer is calculated by the following expression

$$\dot{n}_{CH_4,exref} = \frac{Q_{FC,ex}}{\Delta\overline{H}_{ref}} \left[\frac{kmol}{s}\right] \tag{12}$$

where $\Delta\overline{H}_{ref}$ is the steam reformation enthalpy of reaction [kJ kmol^{-1}] and $Q_{FC,ex}$ [kW] is the amount of heat taken from the fuel cell exhaust stream. As previously stated, the external reformer exhaust composition is assumed to be the equilibrium composition at the resulting temperature. Therefore, the amount of hydrogen yield depends strongly on the position of the external reformer since it determines the amount of available heat from the fuel cell exhaust that can be taken without hindering fuel cell thermal balance. In addition to the amount of heat transferred, hydrogen yield depends on the temperature at which the reaction takes place. In all configurations, the steam-to-carbon ratio (S/C) is equal to 2.

3.5. Heat exchangers (fuel, water and steam preheaters)

The fuel cell plant contains three heat exchangers that preheat fuel, water and air to the input temperature (1173 K). All the heat exchangers are assumed to be counter-flow. The pinch-point or minimum temperature difference considered to avoid temperature crossovers within the heat exchanger is $\Delta T_{min} = 40$ K

Heat exchangers have been analyzed using the *Effectiveness-NTU Method* [16] where effectiveness ϵ has been defined as

$$\epsilon = \frac{C_h(T_{h,i,} - T_{h,o})}{C_{min}(T_{h,i} - T_{c,i})} \tag{13}$$

where C[kW/K] is the product of the fluid specific heat [kJ/kmol·K] and the molar flow rate [kmol/s] and. T is temperature. Finally, the actual heat transfer q may be determined from the expression

$$q = \epsilon C_{min}(T_{h,i} - T_{c,i}) \tag{14}$$

As mentioned, in order to not compromise the fuel cell thermal balance, fuel, steam and air temperatures have been fixed to the following values

$$T_{c,o,fuel} = 1173 \text{ K} \tag{15}$$

$$T_{c,o,water} = 1173 \text{ K} \tag{16}$$

$$T_{c,o,air} = 1173 \text{ K} \tag{17}$$

Equations (13)–(17) form a set of expressions that allows the

determination of the stream temperatures. The state points for all the heat exchangers, including the heat exchanger that links the external reformer and the fuel cell exhaust stream are resolved simultaneously.

3.6. Hydrogen separation and purification

Hydrogen separation and purification in refineries has been traditionally accomplished by using established technologies such as Pressure Swing Adsorption (PSA), selective permeation processes using polymer membranes, or cryogenic separation process. Each process is based on a different separation principle, so each method differs significantly from each other. Economic aspects and other project considerations such as process flexibility, reliability, and scalability have to be taken into account to decide the hydrogen separation method [17].

Other hydrogen separation technologies include Electrochemical Hydrogen Separation (EHS), which is foreseen as a promising technology to separate hydrogen fuel from a fuel cell anode exhaust stream. However, EHS technology is not currently mature and has not been used in polygenerating applications to-date. Thus, analyzing the performance of polygenerating HTFC with EHS is not considered herein, but is rather left to future work.

In the current study, the hydrogen-rich stream is prepared and purified in the Hydrogen Separation Unit (HSU) that relies upon PSA technology due to its commercial readiness [18] and recent use in polygenerating systems. In the external reformation cases, the HSU is placed downstream of the external reformer, as observed in Figs. 2–6. In the internal reformation configurations, unused hydrogen is separated from the anode-off-gas in the Hydrogen Separation Unit (HSU) block, as shown in Fig. 7.

The main purpose of the HSU is to prepare the hydrogen-rich gas stream for the separation process (i.e., PSA), and purify the hydrogen for its use in other applications (i.e., fuel cell vehicles). Additionally, the HSU is used to recover as much heat as possible to maintain the overall plant thermal balance.

3.6.1. Hydrogen separation unit (HSU) model

The HSU configuration depends upon the specific requirements of the hydrogen separation technology and the anode-off-gas conditions. PSA technology requires relatively low inlet temperatures and high inlet pressures. In the internal reformation configurations (6a/b), hydrogen-rich gas (anode-off-gas) is usually available at relatively high temperatures and low pressures. Additionally, hydrogen separation with PSA becomes more efficient at high hydrogen partial pressures [17]. Therefore, to extract the hydrogen from the anode-off-gas of an SOFC using a PSA, the HSU is required to:

- Decrease the anode-off-gas temperature
- Increase the anode-off-gas pressure
- Increase the hydrogen partial pressure

Table 1 shows representative PSA feed gas requirements and the current configuration design points.

In the current study, a simplified HSU block has been modeled with Aspen Plus® and integrated into the SOFC polygeneration system model. As shown in Fig. 8, a series of heat exchangers and compressors have been included to meet the PSA temperature and pressure requirements.

As shown in Fig. 8, an electric chiller has been placed upstream of the PSA reactor to meet the temperature requirements when ambient air temperatures (used as a cold media in the heat exchangers) are too high. The electric chiller represents only a small parasitic load since most of the required cooling is provided by the ambient air heat exchangers. Interestingly, required PSA inlet temperature is low enough to condense out sufficient water vapor from the gas stream. As shown in Fig. 8, condensed water is removed upstream of the PSA reactor resulting in higher hydrogen partial pressure and easing the PSA separation process. It is important to note that the air and water that is heated in the HSU is used in the fuel cell plant as part of the overall thermal integration strategy of the system in each case. HSU performance results are presented in more detail in section 4.4.

4. Results and discussion

The main objective of this work is to investigate and compare the performance of each polygenerating HTFC configuration in order to define the best strategy/approach for polygenerating electricity, hydrogen and heat.

4.1. Bulk stack and external reformer temperatures

For the external reformation cases, the heat available to produce hydrogen without compromising the thermal balance of the fuel cell determines how much methane will be taken by the external reformer according to Eq. (9). However, the hydrogen yield will be a function of the temperature at which the reformation takes places. As shown in Fig. 1, hydrogen yield peaks between 900 K and 1000 K and it flattens out after this point. Therefore, the external reformer should operate in this temperature range in order to maximize the hydrogen production.

Fig. 9 shows both fuel cell stack and external reforming temperatures for all the configurations. As expected, stack temperatures are equal for all cases since inlet stream temperatures have been fixed to a certain value. Importantly,

Table 1 – State-of-the-art PSA feed gas requirements and design point.

Parameter	State-of-the-art value range	Design point	Notes
Absolute Pressure [kPa]	303–2026	1013.15	Based on the state-of-the-art [20]
Temperature [°C]	4–50	25	Based on the state-of-the-art [20]

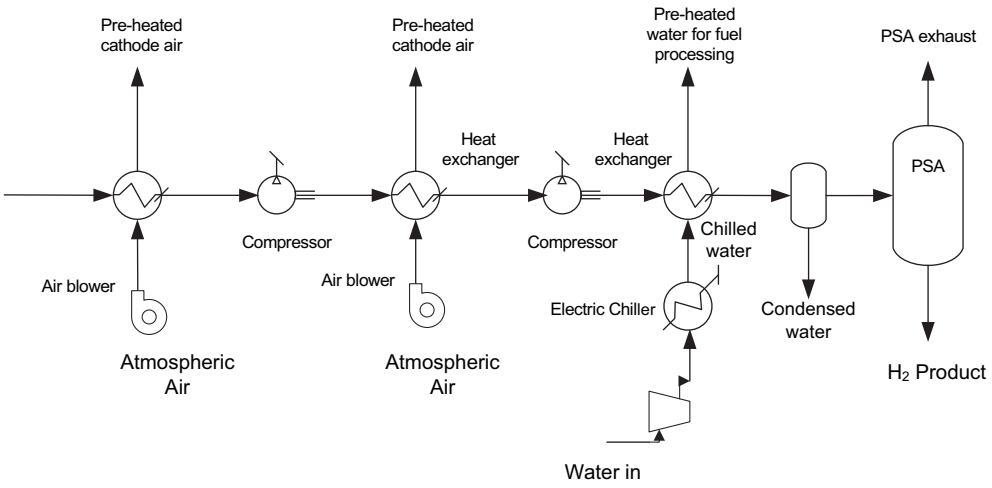

Fig. 8 – Hydrogen Separation Unit Configuration.

in configurations 6a and 6b, stack and reformation temperatures are equal due to the fact that hydrogen is produced internally in the stack by internal reforming.

Configuration 1 presents the lowest reformation temperature. This makes sense since the external reformer is placed downstream all the heat exchangers where exhaust gas temperatures are lowest. Configuration 3b achieves the highest reformation temperature among all configurations. This configuration is the only external reforming configuration where the fuel utilization factor has been lowered to 60%. Therefore, more hydrogen will be oxidized in the catalytic combustor raising the exhaust gas temperature considerably. The rest of the configurations present similar reformation temperatures values, all of them in range where hydrogen yield is maximized.

4.2. *Reversible cell voltage*

Fig. 10 shows the reversible ideal voltage E_0 and the Nernst potential V_{Nervst} of each configuration. As expected from Eq. (4), E_0 is equal for each configuration since the change in Gibbs free energy $\Delta g_f(T)$ is only a function of temperature. However, V_{Nernst} is higher in configurations where the fuel utilization factor (U_F) is lower (i.e., configurations 3b and 6b) due to the fact that it depends not only upon the temperature but also on the product and reactant concentrations.

Despite the importance of the effects of polygeneration on the electrochemical behavior of the fuel cell, cell polarizations are not included in this analysis since these results are only used for comparatives analyses between similar systems. Nevertheless, an in-depth analysis of the effects of polygeneration upon the electrochemical cell performance was investigated by Margalef on his work on polygenerating HTFC [19].

4.3. *Hydrogen production rate*

Fig. 11 shows the amount of hydrogen produced with each configuration. As observed, there is a significant difference between the hydrogen produced with the external reforming configurations and the amount of hydrogen produced with the internal reformation configurations.

The amount of hydrogen produced with configuration 1 is almost negligible. As shown in Fig. 9, the temperature at which reformation occurs in configuration 1 is 724 K whereas at this temperature, the hydrogen yield in equilibrium conditions is very small (see Fig. 1).

Fig. 9 shows in configurations 2, 3a, 3b and 4, external reforming occurs at temperatures at which hydrogen yield is

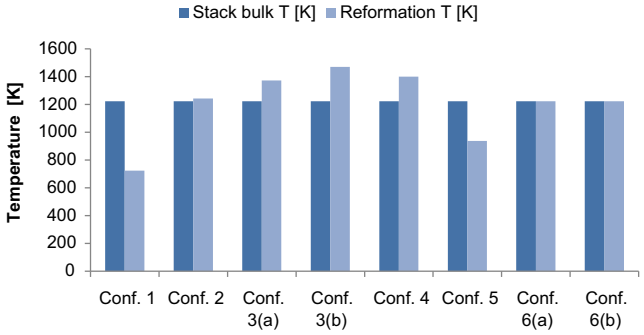

Fig. 9 – Stack and Reformation Temperatures.

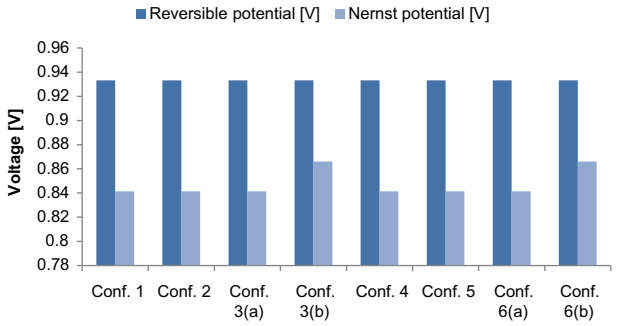

Fig. 10 – Reversible and Nernst potential.

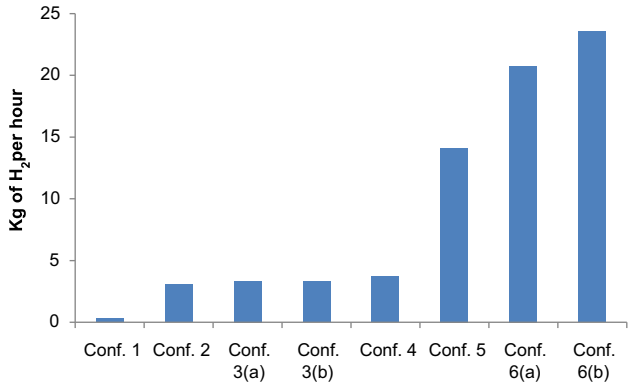

Fig. 11 – Hydrogen production after PSA.

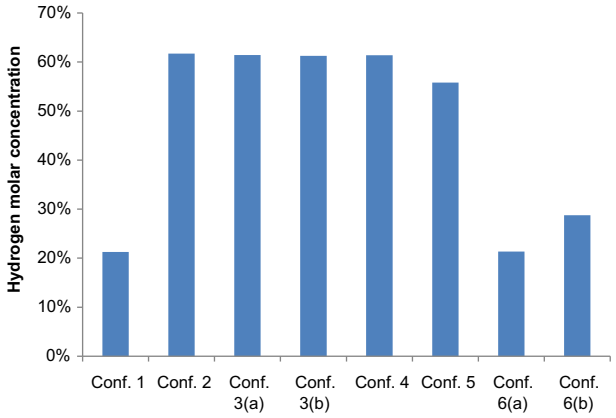

Fig. 13 – Hydrogen concentration in the PSA feed gas.

maximized. However, the amount of hydrogen produced is not comparable to the internal reformation cases or configuration 5. As mentioned, hydrogen production is a function of the temperature at which the reformation occurs but also a function of the amount of transferred heat from the exhaust gas stream to the external reformer $Q_{FC,ex,}$. Although in configurations 2, 3, and 4, steam reforming occurs at relatively elevated temperatures, the heat that can be transferred from the fuel cell exhaust to the reformer without compromising the fuel cell thermal balance is not enough to reform large amounts of methane. As a result, the amount of hydrogen that can be produced with these configurations is not very significant.

Configuration 5 presents higher hydrogen production than the previous external reforming configurations. In this case, since the external reformer is placed after the catalytic combustor, the temperature at which the reformation occurs is high enough to achieve significant hydrogen yields. Importantly, since there is not any preheater downstream of the reformer, more heat can be extracted from the fuel cell exhaust stream without affecting any fuel cell stream input temperature.

Finally, configurations 6a and 6b achieve the highest hydrogen production. This is due to the fact that the reformation takes place within the SOFC stack which operates between the range of temperatures in which hydrogen is maximized. Additionally, the reformation reactions and the fuel cell reactions occur in the same physical space. Therefore, heat from the source (i.e., exothermic fuel cell reactions) to the sink (i.e., endothermic reformation reactions) is directly transferred without the need of a heat exchanger. Thus, more heat can be captured resulting in higher hydrogen yields. The total hydrogen production for each configuration is shown in Fig. 11.

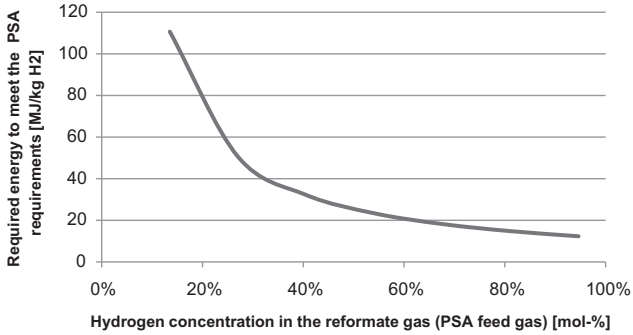

Fig. 12 – Specific energy required for the PSA process.

4.4. *Parasitic loads associated with the hydrogen separation*

In this work, the energy required to separate the hydrogen from the reformate stream in each configuration has been estimated. Pressure Swing Adsorption (PSA) has been the technology selected to separate and purify the hydrogen from the reformate gas. PSA requires high pressure and low temperature feed gas. Table 1 shows the state-of-the-art PSA temperature and pressure requirements and the designated values for this analysis.

The Hydrogen Separation Unit (HSU) is required to increase the pressure and drop the temperature of the reformate gas in order to meet the PSA requirements. This process requires energy and as a result, decreases the overall efficiency of the polygenerating plant. To investigate the energy penalty associated with the separation of hydrogen, a simplified HSU model has been built with Aspen Plus® [21]. The amount of

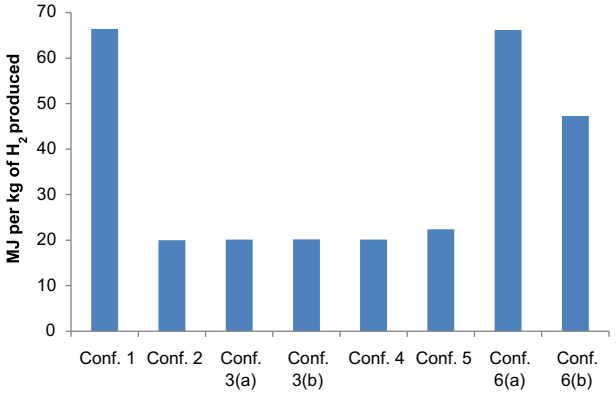

Fig. 14 – Energy required by the HSU to separate one kg of H_2

Table 2 – Efficiency Equations ((1) State-of-the-art Method; (2) Ideal polygeneration Method; (3) Supplemental Input Method).

		Electrical Efficiency	Thermal Efficiency	Hydrogen Efficiency	Total Mixed Efficiency
1		$P_{net}/E_{tot} - \frac{Q_{net}}{\eta_{boiler}} - \frac{H_2}{\eta_{SMR}}$	$Q_{net}/E_{tot} - \frac{P_{net}}{\eta_{CC}} - \frac{H_2}{\eta_{SMR}}$	$H_2/E_{tot} - \frac{P_{net}}{\eta_{CC}} - \frac{Q_{net}}{\eta_{boiler}}$	$P_{net} + Q_{net} + H_2/E_{tot}$
2		$P_{net}/E_{tot} - Q_{net} - H_2$	$Q_{net}/E_{tot} - P_{net} - H_2$	$P_{PSA}/E_{tot} - P_{net} - Q_{net}$	$P_{net} + Q_{net} + H_2/E_{tot}$
3	External Reforming	$P_{net}/E_{tot} - \frac{Q_{e^-}}{\eta_{boiler}} - (F_{H_2} + (P_{PSA}/\eta_{CC}))$	$Q_{net}/(Q_{net}/\eta_{boiler}) = \eta_{boiler}$	$H_2/F_{H_2} + (P_{PSA}/\eta_{CC})$	$P_{net} + Q_{net} + H_2/E_{tot}$
	Internal Reforming.	$P_{net}/E_{tot} - \frac{Q_{e^-}}{\eta_{boiler}} - ((U_F - U_{F,H2ES})E_{tot} + (P_{PSA}/\eta_{CC}))$		$H_2/(U_F - U_{F,H2ES})E_{tot} + (P_{PSA}/\eta_{CC})$	

energy required to separate 1 kg of hydrogen as a function of the hydrogen concentration in the reformate gas has been estimated. The HSU model consists of a series of heat exchangers and compressors that decrease the temperature and increase the pressure of the reformate gas to the design point levels, accordingly, for each configuration. Fig. 12 shows the energy per kilogram of hydrogen required for the preparation of the reformate gas to meet the PSA requirements, as a function of the molar concentration of hydrogen.

As seen, the energy required to separate 1 kg of hydrogen from the reformate stream does not decrease linearly with the hydrogen molar concentration and it can be described by the following curve fit

$$E_{H_2HSU} = 11.613 x_{H_2}^{-1.123} \left[\frac{MJ}{kg\ H_2}\right] \quad (18)$$

where x_{H2} is the hydrogen concentration in the reformate stream. As seen, the amount of energy required to separate the hydrogen from the reformate gas depends upon the hydrogen concentration in the anode-off-gas. This is due to the fact that for lower hydrogen concentrations, relatively more gas has to be compressed to produce less hydrogen. Therefore, the amount of energy required to separate 1 kg of hydrogen with PSA technology is lower when the hydrogen concentration of the feed gas is high. Fig. 13 shows the molar hydrogen concentrations of the PSA feed gas for each configuration.

Hydrogen concentrations remain around 60% for all of the external reformation configurations except for configuration 1. Although the heat available to produce hydrogen in configuration 1 is comparable to the rest of the configurations, the temperature at which the reformation occurs is not high enough to achieve significant methane conversion rates. Similarly, configurations 6a and 6b present low hydrogen concentrations compared to the rest of the configurations. This makes sense since the produced hydrogen is mixed with the anode-off-gas products which include all the carbon dioxide and steam products from the stack reactions, including internal reforming and electrochemical reactions. As a result, the hydrogen concentration of the reformate gas for the internal reformation cases is relative low when compared with the external reformation configurations.

Fig. 14 shows the energy required to separate 1 kg of hydrogen with each configuration. As seen, higher hydrogen concentration streams require less energy to separate the hydrogen from the reformate gas.

4.5. *Efficiency results*

Because a polygenerating HTFC simultaneously produces electricity, hydrogen and useful thermal energy, efficiencies can be measured and expressed in a number of different ways. Margalef et al. developed three different methods to appropriately calculate the overall and coproduct production efficiencies [8]. Table 2 shows the developed equations for each method. The methods have been labeled as: (1) *State-of-the-art Method*; (2) *Ideal Polygeneration Method*, and (3) *Supplemental Input Method*.

These methods are based upon different and reasonable assumptions. It should be clear that there is not a unique solution and that each of the methodologies proposed can be used in comparative analyses if based upon truthful assumptions [7]. For this specific analysis, the *Supplemental Input Method* is used to estimate the overall, electrical and hydrogen efficiencies for each configuration. Thermal efficiency has not been calculated since it depends upon each specific application and there may be cases when thermal energy is not required. Results are presented in Table 3.

The efficiency results shown in Table 3 correspond to the Supplemental Input Method developed to calculate the efficiencies of different polygenerating HTFC configurations [7]. It has to be clear that these results do not include the heat products shown in the equations presented in Table 2.

Table 3 – Efficiency Results obtained with the Supplemental Input Method (LHV).

Configuration	1	2	3a	3b	4	5	6a	6b
Electrical Efficiency	53.4%	53.3%	53.3%	46.9%	53.3%	52.8%	50.0%	58.4%
Hydrogen Efficiency	18.0%	73.5%	73.2%	68.2%	73.2%	62.1%	90.7%	83.5%
Overall Efficiency	52.3%	54.7%	54.8%	48.5%	55.0%	55.7%	70.0%	69.5%

With this method, electrical efficiency is the net power output p_{net} divided by the energy flow allocated exclusively for the electricity production, which corresponds to the total energy flow in E_{tot} minus the energy flow that has been specifically used to produce hydrogen product. The energy flow used to produce hydrogen product includes feedstock energy (i.e., additional fuel) as well as the necessary fuel to generate the electricity required for the hydrogen separation as if it was produced with a state-of-the-art combined cycle plant. The lowest electrical efficiency value corresponds to configuration 3b. In this case, hydrogen is produced externally and the fuel cell is operating at 60% utilization factor. As expected, the electrical efficiency is low since more fuel is used without obtaining any additional energy flow output (i.e., hydrogen fuel). On the other hand, the highest electrical efficiency value corresponds to configuration 6b, in which hydrogen is produced internally and the fuel cell is operated at 60% utilization factor. Due to synergism associated with higher voltages at lower fuel utilizations, electrical efficiency is significantly higher than the rest of the configurations. Nevertheless, this analysis demonstrates that these synergies are only captured if hydrogen is separated from the anode-off-gas. Otherwise, more fuel is being used to obtain the same energy mix outputs. The rest of configurations present similar electrical efficiencies.

With the Supplemental Input Method, hydrogen efficiency is calculated in a similar way. The chemical power output of the hydrogen produced H is divided by the energy flow input specifically allocated to produce hydrogen. Once again, it corresponds to the feedstock energy (i.e., additional fuel) as well as the necessary fuel to generate the electricity required for the hydrogen separation as if it was produced with a state-of-the-art combined cycle plant. As seen in Table 3, the highest values correspond to the internal reformation cases. Interestingly, although the parasitic load per kilogram of hydrogen is higher in configuration 6a than in configuration 6b (see Fig. 14), hydrogen efficiency is greater in the former case due to the fact that when hydrogen is operating at 80% utilization factor, the additional fuel feedstock allocated to produce hydrogen is equal to zero.

Finally, overall efficiency values are similar in all the external reformation cases, even for configuration 1 where the hydrogen output is almost negligible. This indicates that the hydrogen production does not affect the overall performance when the amount of hydrogen is relatively small (i.e., external reformation cases). As expected, both internal reformation cases achieve the highest overall efficiency values.

5. Conclusions

Multiple configurations of polygenerating SOFC have been analyzed. These configurations include electricity, heat and hydrogen production by various methods in the cycle: via an external reformer that captures fuel cell waste heat from different locations and via internal reforming. From all the performed analyses, it is concluded that the highly integrated and synergistic nature of producing additional hydrogen by internal reformation results in the highest electricity and hydrogen production efficiencies. On the other hand, when hydrogen is produced via an external reformer, it is not trivial to transfer the heat from the fuel cell to the external reformer at a high enough temperature to produce significant amounts of hydrogen without compromising the overall system performance.

REFERENCES

[1] Yildiz B, Kazimi MS. Efficiency of hydrogen production systems using alternative nuclear energy technology. Int J Hydrogen Energy 2006;31:77–92.
[2] California Fuel Cell Partnership. Hydrogen fuel cell vehicle and station deployment plan: a strategy for meeting the challenge ahead- Action Plan; 2009.
[3] Bossel U. Energy and the Hydrogen Economy; 2003.
[4] Intergovernmental Panel on Climate Change (IPCC). Climate change 2007 – the physical Science basis. Cambridge, United Kingdom: Cambridge University Press; 2007.
[5] Brouwer J, Leal E. Production of hydrogen Using High-Temperature Fuel Cell: Energy and Exergy Analysis", 18th International Congress of Mechanical Engineering, ABCM; 2005.
[6] Brouwer J, Leal E. A thermodynamic analysis of electricity and hydrogen polygeneration using a solid oxide fuel cell. J Fuel Cell Sci Tech 2006;3:137–43.
[7] Margalef P. On the Polygeneration of Electricity, Hydrogen, and Heat with High Temperature Fuel Cells. Ph.D. dissertation, G.S. Samuelsen, advisor, University of California, Irvine 2010.
[8] Margalef P, Brown T, Brouwer J, Samuelsen GS. Efficiency of polygenerating high temperature fuel cells. Journal of Power Sources 2011;196(4):2055–60.
[9] Shaffer B, Hunsuck M, Brouwer J, Quasi-3D dynamic model of an internally reforming planar solid oxide fuel cell for hydrogen co-production. In: Proceedings of the 6th International Fuel Cell Science, Engineering and Technology Conference. June 16–18, 2008, Denver, Colorado, USA 2008.
[10] Panapoulos KD, Frida L, Karl J, Poulou S, Kakaras E. High temperature solid oxide fuel cell integrated with novel allothermal biomass gasification Part I: modeling and feasibility Study. J Power Sources 2006;159:570–85.
[11] Ohtsuki J, Seki T, Miyazaki M, Sasaki A. Development of Indirect internal reforming molten carbonate fuel cell. Electr Eng Jpn 1992;115(3).
[12] Carstensen JH, Beglid-Hansen J. New developments in shift catalyst for ammonia. Hydrocarbon Processing 1990;69(3): 57–62.
[13] Singhal SC, Kendall K. High temperature solid oxide fuel cells: fundamentals, design and applications. Oxford, UK: Elsevier Advanced Technology; 2003.
[14] O'Hayre R, Cha S, Colella W, Prinz FB. Fuel cell Fundamentals. New York, NY: John Wiley & Sons; 2006.
[15] Gordon S, McBride BJ. NASA RP 1311, Computer Program for Calculation of Complex Chemical Equilibrium Compositions and Applications I. Analysis; 1994.
[16] Incropera F, DeWitt D. Fundamentals of heat and Mass transfer. 5th ed. John Wiley & Sons; 2001.
[17] Miller QM, Stocker J. Selection of a hydrogen separation process," NPRA Annual Meeting held March 19–21, 1989.
[18] Heydorn EC, Patel P. Development of a Renewable Hydrogen Station, International Colloquium on Environmentally Preferred Advanced Power Generation (ICEPAG) February 9th–11th Costa Mesa, CA 2010.
[19] Margalef P. On the polygeneration of electricity, heat and hydrogen with high temperature fuel cells, PhD dissertation, University of California, Irvine 2010.

[20] Air products & chemicals Inc., Recovery process using pressure swing adsorption technology, Available online at: http://texasiof.ces.utexas.edu/texasshowcase/pdfs/presentations/c6/pcook.pdf.
[21] Aspen Plus. Aspen Plus® User Models. Cambridge, MA: Aspen Technology Inc.; 2006.

Glossary

DIR: Direct internal reformation
EHS: Electrochemical Hydrogen Separation
GW: Gigawatt
HSU: Hydrogen separation unit
HTFC: High temperature fuel cell
kW: Kilowatts
kWh: Kilowatt-hour
LCA: Life cycle analysis
LHV: Lower heating value
MCFC: Molten carbonate fuel cell
PSA: Pressure swing adsorption
S/C: Steam-to-carbon ratio
SMR: Steam methane reformation
SOFC: Solid oxide fuel cell
WGS: Water-gas shift
WTT: Well-to-tank
Q: Heat flow rate [kW]
μ: Chemical potential
E: Energy flow rate [kW]
ϵ: Effectiveness
E_o: Open circuit voltage
F: Faraday's constant
F: Fuel flow rate [kW]
g_f: Gibbs free energy of formation
H: Enthalpy
H_2: Hydrogen flow rate (on LHV basis) [kW]
$\dot{n}$: Molar flow rate
P: Electric power
P: Pressure
p: Partial pressure
Q: Heat flow rate [kW]
R: Gas constant
T: Temperature
U_f: Fuel utilization factor
$U_{f,\ H2ES}$: Fuel utilization factor on polygeneration mode
V: Voltage
W: Work
w: Specific work
z: Number of electrons released during oxidation
η: Efficiency
$\dot{m}$: Mass flow rate

Subscripts
h: Hot stream
c: Cold stream
i: Inlet
o: Outlet
min: Minimum
x: Stream: Fuel (f), water (w) and air (a)
cc: Combined cycle
tot: Total
e^-: Electricity production
FC: Fuel cell
ex: External
Ex ref: External reformation
HSU: Hydrogen separation unit